Effect of Minor Elements on Hot-Cracking Tendencies of Inconel 600

Minor-element additions, incorporated into welds by a powder-metallurgy-insert technique, have a significant effect on hot-cracking propensity as evaluated by a subscale Varestraint Test

BY W. F. SAVAGE, E. F. NIPPES AND G. M. GOODWIN

ABSTRACT. An investigation was undertaken to determine the effect of six minor elements, S, P, Si, Mn, Ti and Al, on the hot-cracking propensity of Inconel, a solid-solution strengthened nickel-base alloy.

In order to determine the effects of these six elements, a new weldability evaluation test, the "Tigamajig" test, was developed. An outgrowth of the "Varestraint" test, the Tigamajig test combines the advantages of its predecessor with a reduced specimen size and ease of specimen preparation. A technique was used which allowed the preparation of a large number of specimens of systematically varied composition by the incorporation of compacted-and-sintered powder inserts containing the desired minor-element additions.

A full factorial experiment was then performed, utilizing all of the 64 possible combinations of the six intentionally added minor elements. The entire testing program was duplicated at two levels of augmented strain to give an accurate estimate of error.

With the aid of the method of Yates and the analysis of variance, the significant effects of the six minor elements were determined for three cracking parameters: the total crack length, the maximum crack length, and the average crack length.

Sulfur and P were found to be highly detrimental to all three of the cracking parameters. The effect of S and P was attributed to a high degree of segregation, and subsequent reduction in the effective solidus and liquidus, coupled with a decrease in the solid-liquid interfacial energy, which permitted wetting of the grain and subgrain boundaries and the subsequent formation of grain-boundary films.

Manganese and Si were both found to reduce the detrimental effect of S, at least in part as a result of an increase in the solid-liquid interfacial energy. However, a significant Si-Mn interaction effect indicated that these elements were not as effective at reducing the effect of S when both were present together.

Titanium and Al also both had beneficial effects on hot-cracking propensity. It was proposed that the effect of Ti and Al, and in part the effect of Mn and Si, was caused by the excellent deoxidizing capabilities of these four elements.

Introduction

The hot-cracking susceptibility of an alloy is dependent upon its elemental composition, and upon the distribution of these elements within the material. Thus, even if two heats of material could be produced with precisely the same overall composition (an impossibility in itself), these materials would not necessarily exhibit similar hot-cracking tendencies because of variations in the solute distribution. This distribution is dependent upon the entire past history of the material, from the time the alloy was cast as an ingot, to the time that the welding is actually performed.

Thus, it is futile to attempt to assign a meaningful cracking-susceptibility index to a particular alloy. However, one may attempt to explain the heat-to-heat variations for a given alloy, and eventually conclusions may be drawn as to how to control the cracking susceptibility of that alloy.

The Varestraint test[1] was developed at Rensselaer as a "universal" weldability test. This test was designed to permit independent control of the welding input parameters used during testing and the degree of restraint to which the specimen is subjected. The "degree of restraint" was simulated by the application of a controlled augmented strain during welding. Thus, it was possible to use welding input variables which were similar to those used in commercial processes, and yet provide any desired level of restraint in a laboratory-scale specimen.

Over the years, the Varestraint test has proven capable of discerning heat-to-heat variations in a large variety of materials.[1,2] In fact, the Varestraint test has been so successful, that it seemed appropriate to employ a similar concept in a large-scale factorial experiment in order to study both the effects of individual elements and the interaction effects of many elements at once.

Obviously, a testing program of this type naturally requires a large number of samples with a considerable number of compositional variations. This becomes a problem with the original Varestraint test because of the consid-

W. F. SAVAGE is Professor of Metallurgical Engineering and Director of Welding Research, and E. F. NIPPES is Professor of Metallurgical Engineering, Rensselaer Polytechnic Institute, Troy, N. Y. G. M. GOODWIN, former Graduate Research Assistant at RPI, is now with the Metals and Ceramics Div., Oak Ridge National Laboratory, Oak Ridge, Tenn.

erable expense required to produce a large number of heats of material and fabricate sufficient samples for Varestraint testing of each heat.

Therefore, a sub-scale test based on the augmented-strain concept was devised to utilize small, readily produced specimens whose composition could be varied as desired.

This test was then used in a large-scale, full-factorial experiment to determine the effect of minor elements on the hot-cracking susceptibility of Inconel 600.

Object

The objective of this experiment was to investigate the basic mechanisms involved in the phenomenon of weld-metal hot-cracking in Inconel 600, and to determine the effect of six minor elements, normally present in this alloy, (S, P, Si, Mn, Ti, and Al) on these mechanisms.

Materials and Apparatus

Preparation of the Basic Ternary Alloy

High-purity (99.9+%) Fe, Cr, and Ni powders were mixed in proportions corresponding to the basic ternary composition of Inconel and consolidated into 4 in. (102 mm) diam. rods, each 24 in. (610 mm) long, by air induction melting and casting in graphite molds. These rods were then welded together and vacuum consumable arc melted into 6 in. (152 mm) molds.

The resulting three ingots were then hot extruded into sheet bar and rolled into ¼ in. (6.35 mm) plate. This sheet bar was initially hot rolled to 5/16 in. (7.9 mm), followed by cold reduction of 20% to final thickness.

The basic ternary material was prepared at Oak Ridge National Laboratory and was delivered to Rensselaer in the form of plates, each 6 × 6 × ¼ in. (152 × 152 × 6.3 mm). The composition of this material is given in Table 1.

Table 1—Composition of High-Purity "Ternary" Base Material, wt-%

Fe	11.6	Ti	0.02
Cr	15.2	Al	0.03
Ni	72.8	C	0.003
S	0.004	Cu	0.014
P	0.001	H_2	0.0004
Si	0.06	N_2	0.004
Mn	0.064	O_2	0.026

Table 2—High Level Aim Composition After Remelting, %

S	0.015	Mn	1.0
P	0.015	Ti	0.5
Si	0.5	Al	0.5

Preparation of the Modified Alloy Pads

To investigate the influence of the six minor elements on hot-cracking propensity, a full-factorial experimental design was chosen.[3] It was chosen to investigate the effects of the six elements at two levels of concentration in all possible combinations.

The high-level aim composition for the six elements is given in Table 2. Since it was impractical to produce the 64 alloys required by remelting the basic ternary and preparing 64 "split-heats," a unique method, developed at RPI, was used for producing the experimental alloys.[4]

In this method, the composition of a small volume within each plate of the basic ternary alloy was modified by the following technique:

1. An alloy insert, prepared by compacting and sintering an appropriate mixture of suitable high-purity powders was inserted in a pre-machined groove along the centerline of the 6 × 6 in. (152 × 152 mm) specimens, as indicated by dashed lines in Fig. 1.

2. A series of three wide-weave GTA welding passes (sinusoidal weave pattern with ½ in. (12.7 mm) peak-to-peak oscillation) were then made to melt and mix the insert with an appropriate volume of the basic ternary alloy. Thus, the resulting specimen contains a remelted "pad" of modified composition with a reproducible pattern of microsegregation typical of a weld deposit made under controlled conditions. The solid lines in Fig. 1 represent the typical appearance of a specimen after the GTA remelting operation.

3. Atmospheric contamination was minimized by performing the GTA remelt operation in a high-purity Ar atmosphere within a dry-box. Contamination by refractory or mold materials is impossible since the entire remelted zone is contained within the basic ternary plate, which thus acts, in effect, as a "crucible."

After the inserts had been GTA remelted into the base-metal plates, the plates were mechanically straightened, sectioned, and drilled, to provide five test specimens with the dimensions shown in Fig. 1.

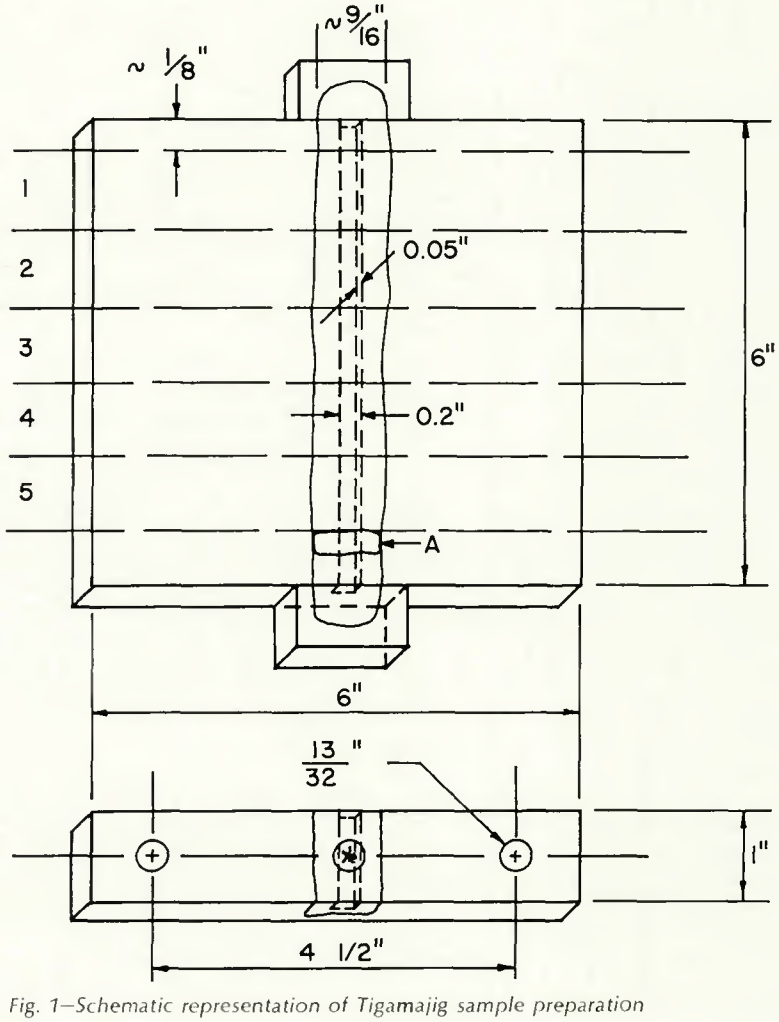

Fig. 1—Schematic representation of Tigamajig sample preparation

Both the top and bottom surfaces of each sample were then fly-cut to assure constant cross-section and to remove surface oxide. Sample thickness was maintained in a narrow range, nominally 0.250 in. (6.35 mm). The 13/32 in. (10.3 mm) diam. holes were drilled in such a manner that the center of the weld deposit was located equidistant between the hole centers.

Chemical Analyses

The results of the chemical analyses of typical weld pads are given in Table 3. An asterisk (*) denotes the aim composition of an element. Note, for example, that Insert 1 contains all six factors at their lower levels, Insert 64 contains all six factors at their higher levels, and so on. These compositions may be compared with the desired fusion-zone compositions given in Table 2.

The significance of the above analyses is best seen by looking at a typical distribution of compositions obtained. Figure 2 is a histogram showing the frequency of occurrence of a particular S concentration as a function of % S. Ideally, this distribution would show one half (32) of the samples at 0% S and the other half at the desired nominal composition, 0.015% S.

The average high level of S concentration was then found by taking the average S content of those samples to which S was intentionally added. Similarly, the average lower level of S content is determined from those samples to which S was not intentionally added. The numbers used in these calculations are indicated at the bottom of Table 3. Histograms for other minor-element additions have been presented in a previous paper.[4]

Description of the TIGAMAJIG* Test

In the development of a sub-scale Varestraint testing device, an attempt was made to preserve the desirable features of the original Varestraint device. The major modifications incorporated in the new test were:

1. A reduction in the specimen size.
2. A workable method of imposing suddenly applied, reproducible, augmented strain during the production of a GTA spot weld in the modified composition contained within the remelted pad described in the previous section.

The specimen geometry finally adopted is shown in Fig. 1. Note that it is only 6 in. (152 mm) long by 1 in. (25 mm) wide with a maximum thickness of ¼ in. (6.35 mm). Testing of this type of specimen has been performed successfully on sheet material as thin as 0.060 in. (1.5 mm), but for this experiment, all samples were nominally ¼ in. (6.35 mm) in thickness.

Note from Fig. 1 that several samples with the same composition could be machined from each 6 × 6 × ¼ in. (152 × 152 × 6.4 mm) plate. This permitted replication of two different testing conditions.

The actual testing is accomplished by initiating a stationary GTA weld at the center of the specimen. After allowing sufficient time for the establishment of approximately steady-state thermal conditions, the desired augmented strain is suddenly applied, and the arc current interrupted. The strain is applied by loading the sample in bending as a fixed-end beam, and the approximate longitudinal augmented strain in the outer fibers can be calculated from the relationship:

$$e \cong t/2R$$

where the tangential strain on the top surface of the specimen, ϵ , is given as a function of specimen thickness, t, and bending radius, R.

Because of the thermal conditions produced by the long-duration, stationary GTA weld, and the essentially

A humorously applied nickname adopted for this version of the Varestraint test.

Table 3—Composition of Typical Inconel Weld Pads, wt-%—Asterisk (*) Indicates Element Intentionally Added

Insert	Fe	Cr	Ni	S	P	Si	Mn	Ti	Al	C	Cu
1	9.63	14.8	74.5	0.005	0.001	0.07	0.056	0.02	0.03	0.003	0.016
11	9.54	14.4	74.7	0.020*	0.001	0.07	0.054	0.31*	0.03	0.003	0.016
19	9.92	14.8	74.5	0.004	0.0005	0.23*	0.050	0.01	0.21*	—	0.01
22	9.23	14.5	75.0	0.004	0.001	0.07	0.060	0.35*	0.33*	0.003	0.014
30	9.34	14.8	74.4	0.016*	0.001	0.15*	0.060	0.23*	0.03	0.002	0.014
39	8.97	14.6	73.4	0.004	0.0008	0.30*	1.200*	0.01	0.21*	—	0.01
53	9.99	14.7	72.3	0.022*	0.010*	0.08	1.400*	0.01	0.27*	—	0.01
56	9.55	14.7	74.6	0.014*	0.004*	0.23*	0.050	0.22*	0.03	—	0.01
64	8.76	14.4	74.5	0.013*	0.004*	0.32*	1.400*	0.37*	0.23*	—	0.01
Avg. without element addition	9.95	14.6	73.7	0.004	0.0013	0.072	0.093	0.014	0.03	0.0028	0.012
Avg. with element addition	9.95	14.6	73.7	0.016	0.0097	0.294	1.331	0.32	0.25	0.0028	0.012

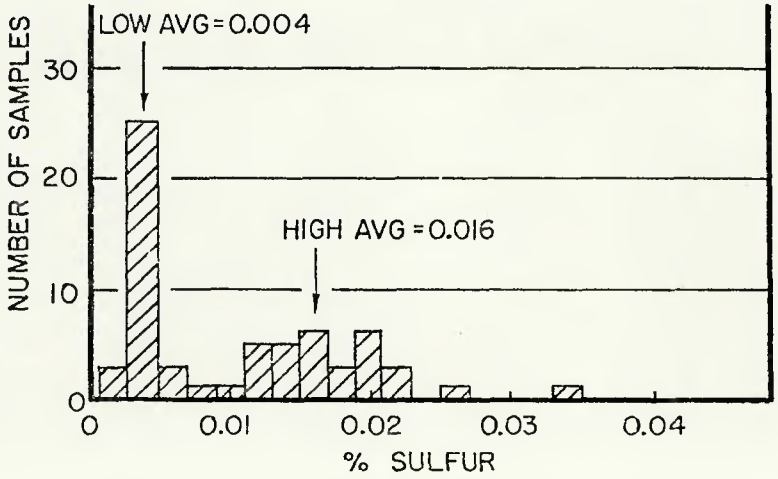

Fig. 2—Distribution of S concentrations in Inconel Tigamajig samples

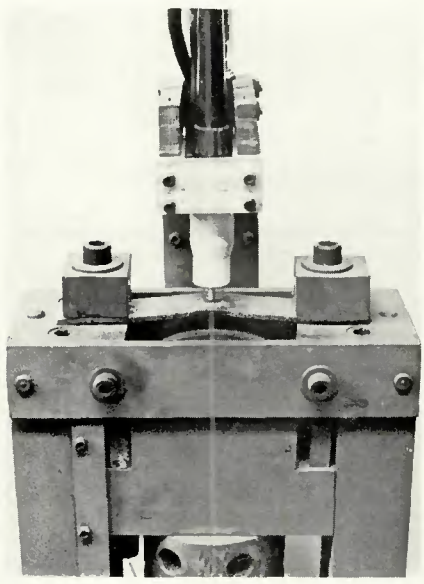

Fig. 3—Photograph of a portion of the Tigamajig test device

transverse orientation of the solidification substructure which already exists in the remelted pad with respect to the augmented strain, the test is extremely sensitive to variations in cracking susceptibility.

The Tigamajig test device is shown in Fig. 3; it consists of four major components—a pneumatic air cylinder, a loading ram and die block assembly, a sample holding fixture, and a torch assembly.

The arc duration and current selected will, of course, depend upon the material under consideration and the specimen thickness; it is desirable to choose these variables such that steady-state thermal conditions are approached before loading occurs. Under such conditions, the transverse thermal gradients established are relatively gradual and the severity of cracking is enhanced. In general, hot cracking occurs over a relatively narrow range of temperatures in the vicinity of the solidus, and a gradual temperature gradient expands the region exposed to the cracking-temperature range at the time of application of the augmented strain.

Procedure

Tigamajig Testing Procedure

The sample-preparation procedure which was discussed in the previous section yielded five essentially identical test specimens of each of the 64 different nominal compositions. The results of this work are based on Tigamajig testing of four of these sets of samples, with the remaining set of samples being utilized to establish suitable test conditions.

All Tigamajig testing was performed under the standard conditions shown in Table 4. Arc current and voltage were continually monitored and maintained to within ±5% of the nominal values reported.

Two nominal levels of augmented strain—1% and 2%—were investigated in the experiment, with two samples being tested at each strain level, thus providing a single replication of the entire experiment. To minimize the effect of systematic errors, the actual order of testing of each of the samples within a set was selected from a table of random numbers.[3]

Immediately prior to testing, each sample was thoroughly degreased with acetone. Shielding gas was allowed to prepurge for at least 30 s before the automated sequence was initiated, and the delay time between samples was maintained such that the radius die blocks and other parts of the Tigamajig device were not allowed to overheat.

Each of the four sets of 64 samples was tested as a unit, and the data were read from each set before testing began on the following set. To minimize the effect of surface oxidation upon the measurement of cracking parameters, the as-welded surface of each of the specimens was cleaned prior to its measurement with the following pickling solution: 700 parts H_2O, 250 parts conc. (70%) HNO_3, and 50 parts conc. (52%) HF. The samples were immersed in the solution at 130 F (54 C) and swabbed for 1–3 min, followed by a rinse in cold water.

Data Accumulation

The cracking data were measured from the specimen surface using a stereo binocular microscope at a magnification of ×40 and a filar eyepiece with 200 divisions, 0.5 mil (0.013 mm) per division.

Throughout this investigation, the only cracks considered were those which actually touched the fusion boundary between the Tigamajig weld nugget and the weld pad. Referring to the schematic representation of the Tigamajig specimen shown in Fig. 1, note that, to be included in the data, a crack had to touch the circular fusion boundary of the Tigamajig test nugget in the center of the specimen. Thus, crater cracks within the Tigamajig nugget were ignored, as were cracks in remote regions of the weld pad which formed during the GTA-remelting process used to prepare the specimens.

A photomacrograph of a typical Tigamajig specimen, showing numerous hot cracks, is presented in Fig. 4 in the polished-and-etched condition at ×9.5. The plane of polish of this metallographic section is approximately 0.005 in. (0.13 mm) below the original sheet surface. In Fig. 4, the structure of the high-purity base metal is evident at both sides of the wide weave GTA bead. The oscillation patterns in this wide-weave bead, and the epitaxial growth from the base metal can be readily identified. The diameter of the GTA spot weld is clearly delineated by a narrow region of planar growth. Also evident is the epitaxial growth of the spot weld from the wide-weave bead.

In addition, the more rapid cooling during solidification of the GTA spot weld has resulted in a finer subgrain structure than that of the wide-weave bead. The discontinuity at the center of the photomacrograph is a consequence of the shrinkage void which occurred during the solidification of the GTA spot.

The length of each of the fusion-boundary cracks was recorded, so that

Table 4—Standard Conditions for Tigamajig Testing of Inconel

Arc current	90 A dcsp
Arc time	30 s
Arc voltage	11 V
Arc length	1/4 in. (6.4 mm) measured cold
Electrode	1/8 in. (3.2 mm) $EWTh_2$ ground to an incl. angle of 90 deg
Shielding gas	25 cfh (18.9 liters/min.) Ar prepurified grade (99.998% min.)
Power supply	3-phase rectifier

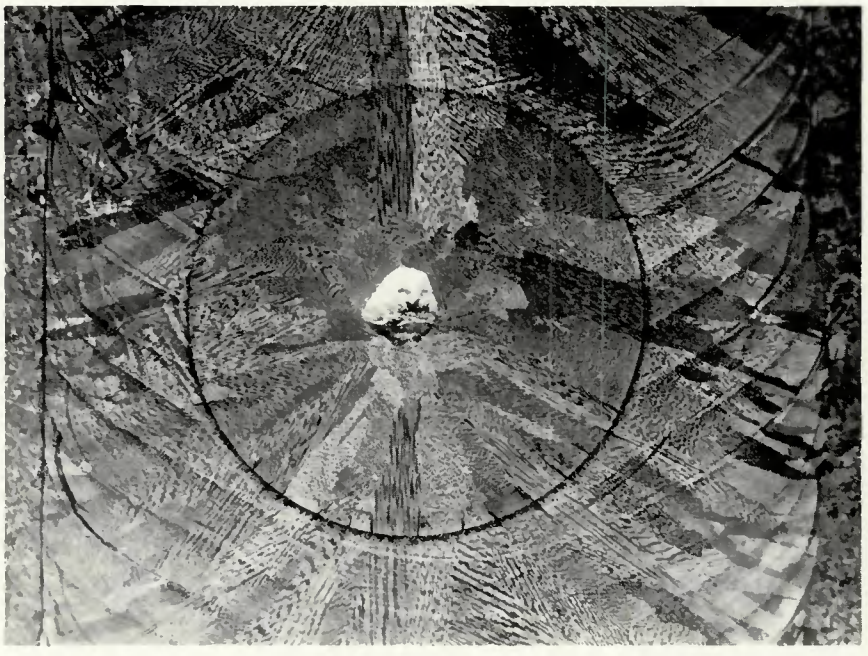

Fig. 4—Example of hot cracking in a specimen tested in the Tigamajig device, polished-and-etched, ×9.5

Table 5—Total Crack Length (TCL), Maximum Crack Length (MCL), and Average Crack Length (ACL) for Inconel Tigamajig Specimens (1% Augmented Strain)

Insert	Alloy additions	Avg. TCL, mils	Avg. MCL, mils	Avg. ACL, mils	Insert	Alloy additions	Avg. TCL, mils	Avg. MCL, mils	Avg. ACL, mils
1		301	16	10	33	P-Si-Mn	362	35	12
2	S	872	194	41	34	Si-Mn-Ti	194	20	10
3	P	524	32	12	35	P-Mn-Ti	174	18	10
4	Si	432	22	10	36	P-Si-Ti	217	26	11
5	Mn	330	20	8	37	P-Mn-Al	329	22	9
6	Ti	206	10	6	38	P-Si-Al	433	28	12
7	Al	304	18	8	39	Si-Mn-Al	242	26	12
8	S-P	951	227	40	40	P-Ti-Al	286	17	8
9	S-Si	636	32	12	41	Si-Ti-Al	202	22	10
10	S-Mn	360	22	10	42	Mn-Ti-Al	149	16	9
11	S-Ti	735	105	19	43	Si-Mn-Ti-Al	184	28	10
12	S-Al	757	93	24	44	P-Mn-Ti-Al	246	20	9
13	P-Si	466	22	10	45	P-Si-Ti-Al	192	21	10
14	P-Mn	294	18	8	46	P-Si-Mn-Al	304	34	16
15	P-Ti	319	17	10	47	P-Si-Mn-Ti	274	24	9
16	P-Al	524	20	10	48	S-Mn-Ti-Al	306	21	10
17	Si-Mn	234	24	10	49	S-Si-Ti-Al	392	24	12
18	Si-Ti	240	26	8	50	S-Si-Mn-Al	247	29	12
19	Si-Al	332	24	10	51	S-Si-Mn-Ti	344	18	8
20	Mn-Ti	155	14	8	52	S-P-Ti-Al	724	84	20
21	Mn-Al	104	14	8	53	S-P-Mn-Al	429	30	12
22	Ti-Al	196	16	8	54	S-P-Mn-Ti	450	26	12
23	S-P-Si	640	174	20	55	S-P-Si-Al	912	117	21
24	S-P-Mn	600	65	15	56	S-P-Si-Ti	840	94	16
25	S-P-Ti	1069	196	35	57	S-P-Si-Mn	446	26	10
26	S-P-Al	962	153	29	58	P-Si-Mn-Ti-Al	214	21	12
27	S-Si-Mn	316	24	11	59	S-Si-Mn-Ti-Al	216	20	9
28	S-Mn-Ti	336	22	9	60	S-P-Mn-Ti-Al	402	22	10
29	S-Ti-Al	468	48	14	61	S-P-Si-Ti-Al	506	53	13
30	S-Si-Ti	555	108	18	62	S-P-Si-Mn-Al	456	26	10
31	S-Si-Al	524	27	11	63	S-P-Si-Mn-Ti	383	22	10
32	S-Mn-Al	316	20	8	64	S-P-Si-Mn-Ti-Al	338	24	11

for each sample, the following parameters were obtained:

1. Total Crack Length (TCL)—The sum of the lengths of all cracks measured in a specimen.
2. Maximum Crack Length (MCL)—The length of the single largest crack observed for a particular specimen.
3. Average Crack Length (ACL)—The length of the average crack in a particular specimen, found by dividing the TCL by the total number of cracks.

To minimize the effects of human error, two observers measured and recorded the cracking data independently for each set of duplicate specimens. The average data obtained for the 1% augmented strain are presented as Table 5 for all 64 test compositions.

Table 6—Summary of Results—Total Crack Length (α = 0.1%)

	Treatment combination	Effect	Best value, mils
1% strain	S	26.5	745
	P	12.6	405
	S-Si	−7.0	675
	Ti	−10.9	170
	S-Mn	−13.1	398
	Mn	−21.6	194
	Mean	—	412
2% strain	S	29.8	1167
	P	14.2	583
	S-Si-Mn	11.2	514
	Si	−13.6	569
	Ti	−14.1	300
	S-Si	−15.2	767
	5-Mn	−16.4	690
	Mn	−20.1	516
	Mean	—	636

Results

The effects which will be discussed were determined by application of the method of Yates, and the significance of these effects was estimated by the analysis of variance.[3,5,6] Only those effects determined to be significant at the α = 0.1% level are considered in the discussion of cracking parameters. This high level of significance was obtained since the entire experiment was replicated, providing an estimate of error based on 64 separate comparisons for each parameter.

Total Crack Length

A summary of the significant effects obtained for total crack length at the two strain levels is shown in Table 6. Note immediately the following generalities: the total crack length at 2% augmented strain shows a 50% increase over the value at 1% strain. This indicates that although the total crack length vs. % augmented strain curve is flattening out, 2% strain is still below "saturation level" for total crack length. This is also attested by the fact that there are more significant effects at 2% than at 1% augmented strain, i.e., it was advantageous to test at the higher strain level as far as the total-crack-length parameter is concerned. However, it is postulated on the basis of past experience that a further increase in strain might cause the total

crack length to approach a saturation value. If this were the case, further increase in augmented strain would not be likely to provide any more information and might, in fact, fail to show some of the effects found significant at the lower augmented strain levels.

To summarize the significant effects on total crack length at both levels of augmented strain:

1. S has a strong detrimental effect.
2. The detrimental effect of S is minimized by the addition of Mn.
3. Si is also beneficial in minimizing the detrimental effect of S.
4. Si and Mn do not work as well in combination as when they are present separately.
5. P is detrimental, especially in the presence of other intentional "impurity" additions.
6. Si and Ti are both beneficial for reducing the total crack length.

Maximum Crack Length

The effects which were determined to be significant on the basis of the maximum crack length are summarized in Table 7.

Before considering the data, some general comments should be made about both levels of augmented strain: there are 16 effects found to be significant at the $\alpha = 0.1\%$ level for 1% strain, while there are only 7 effects significant at the 0.1% level with 2% strain. Note that doubling the strain only caused an increase in the mean maximum crack length from 44 mils to 49 mils. This behavior appears to indicate that above a certain strain level the maximum crack length is more dependent on the thermal gradients which exist in the Tigamajig specimen than on the level of augmented strain. Thus, the maximum crack length proved to be an extremely sensitive indicator of cracking tendencies at the 1% augmented strain level, but less effective at the 2% strain level.

To summarize the effects on maximum crack length:

1. S has a detrimental effect on the maximum crack length.
2. The effect is reduced by the addition of either Mn or Si, with Mn being more effective.
3. The beneficial effect of either Mn or Si is reduced when both elements are present together.
4. P has a detrimental effect, especially in the presence of S.
5. Mn helps to reduce the effect of P.
6. Ti and Al both reduce the maximum crack length, the latter through an interaction with S.

Table 7—Summary of Results—Maximum Crack Length ($\alpha = 0.1\%$)

	Treatment combination	Effect	Best value, mils
1% strain	S	45.4	132
	P	18.4	11
	S-Mn-Al	15.0	13
	S-P	14.7	191
	Si-Mn	14.2	46
	S-Si-Mn	12.8	45
	Si	−12.3	13
	P-Mn	−12.6	42
	S-P-Mn	−12.8	57
	Ti	−13.5	0
	Mn-Al	−15.8	8
	Al	−17.6	39
	S-Al	−17.9	98
	S-Si	−19.4	74
	Mn	−40.5	38
	S-Mn	−41.6	49
	Mean	—	44
2% strain	S	46	171
	S-Si-Mn	30	33
	Si-Mn	30	32
	Si	−24	27
	S-Si	−31	56
	Mn	−39	25
	S-Mn	−44	28
	Mean	—	49

Table 8—Summary of Results—Average Crack Length ($\alpha = 0.1\%$)

	Treatment combination	Effect	Best value, mils
1% strain	S	3.13	27.9
	Si-Mn	1.69	11.4
	S-Si-Mn	1.28	10.1
	P	1.22	11.4
	Si	−1.16	10.1
	Ti	−1.22	6.6
	S-Si	−2.13	15.4
	Mn	−2.69	8.6
	S-Mn	−2.91	10.8
	Mean	—	13.0
2% strain	S	3.1	32.3
	Si-Mn	2.4	15.7
	S-Si-Mn	2.2	13.1
	S-Si	−2.8	17.5
	Mn	−3.0	9.7
	S-Mn	−3.8	9.5
	Mean	—	15.0

Note that doubling the strain only caused an increase in the mean maximum crack length from 44 mils to 49 mils. This behavior appears to indicate that above a certain strain level the maximum crack length is more dependent on the thermal gradients which exist in the Tigamajig specimen than on the level of augmented strain. Thus, the maximum crack length proved to be an extremely sensitive indicator of cracking tendencies at the 1% augmented strain level, but less effective at the 2% strain level.

To summarize the effects on maximum crack length:

1. S has a detrimental effect on the maximum crack length.
2. The effect is reduced by the addition of either Mn or Si, with Mn being more effective.
3. The beneficial effect of either Mn or Si is reduced when both elements are present together.
4. P has a detrimental effect, especially in the presence of S.
5. Mn helps to reduce the effect of P.
6. Ti and Al both reduce the maximum crack length, the latter through an interaction with S.

Average Crack Length

The significant effects on the average crack length are summarized in Table 8. Note that, as was the case for the maximum-crack-length consideration, more significant effects are found at the 1% than at the 2% augmented strain level.

The six effects significant at the $\alpha = 0.1\%$ level for 2% strain are the same as the first six significant effects at 1% strain; thus it appears that the additional strain clouds the issue, decreasing the significance of some effects which appeared at the lower augmented strain level. Note that the mean value of the average crack length only increases from 13 to 15 mils when the strain level is increased from 1% to 2%.

To summarize the effects on the average crack length:

1. S has the strongest detrimental effect.
2. The detrimental effect of S is reduced most efficiently by the presence of Mn.
3. Si is also effective at reducing the detrimental effect of S.
4. As was seen for the case of total crack length and maximum crack length, Si and Mn have an adverse synergistic effect, and thus are less effective in combination than when each element is present separately.

5. P is seen to have a detrimental effect.

6. Ti has a beneficial effect, as was also seen for both of the other cracking parameters.

Discussion of Results

In general, it is seen that all three of the cracking parameters considered are significant indicators of cracking propensity. For this alloy, the maximum crack length at 1% augmented strain appears to be the most sensitive indicator of cracking tendencies, showing at least twice as many effects significant at the $\alpha = 0.1\%$ level as either of the other parameters. Note, however, that coupled with this high sensitivity is a high degree of scatter, so that it would be extremely risky to base conclusions upon only a few measurements of the maximum crack length. In general, if only a few specimens are available, more valid conclusions may be formed from measurements of the total crack length and/or average crack length.

It should be noted that the maximum crack length is highly sensitive to the temperature gradient present at the instant of straining. In fact, it appears that the maximum crack length exhibits a saturation value directly related to the distance from the weld pool to a point where the temperature falls below the effective solidus of the segregated boundary experiencing cracking. Once sufficient augmented strain is imposed to propagate a crack to this point, a further increase in strain has little effect on maximum crack length. Therefore, in all cases, care must be taken to ensure that the testing is performed below this saturation strain level for the material under investigation.

Note also that the saturation strain may have a different value for each of the cracking parameters considered. For example, in this experiment, there was a greater number of significant effects on the total crack length at the 2% than at the 1% augmented strain level, while the opposite was true for both the maximum crack length and the average crack length.

For all three of the cracking parameters considered, S had by far the strongest detrimental effect. Some of the reasons for this strong effect of S may be deduced from the Ni-S binary phase diagram. The addition of S to Ni causes a drastic reduction in both the liquidus and solidus temperatures. Furthermore, the average distribution coefficient*, $k_{avg.}$, is approximately 0.0005. Thus, during solidification, even a weld with an extremely low nominal S content may develop segregated areas which are high in S and therefore have a correspondingly low melting point. Such regions are particularly prone to cracking when subjected to either a thermally induced or an augmented strain at temperatures near or above their effective solidus temperature.

A typical hot crack in a sample containing S as an intentional addition is shown in Fig. 5. This photomicrograph was taken of the etched surface utilizing Normarski phase contrast. The fusion boundary between the Tigamajig nugget on the left and the weld pad on the right is readily evident. Also note that there are second-phase particles, probably oxides, in both the GTA spot fusion zone and the weld pad. The inclusions tend to be located along grain and subgrain boundaries produced during solidification in both instances. Thus, the slow cooling which caused the coarser substructure in the weld pad is probably the explanation for the larger inclusions apparent in this region as well.

The portion of the hot crack within the GTA spot weld in Fig. 5 proceeds along grain and subgrain boundaries, as did all such cracks observed in this investigation. It is in these last regions to solidify that one would expect to find segregated those elements such as S which have a distribution coefficient, k, less than unity. Therefore, this work confirms the classical theory that S causes hot cracking by lowering the liquidus and solidus temperatures of the regions in which segregation occurs.

The detrimental effect of P on cracking might also be anticipated from inspection of the Ni-P binary diagram, which contains a eutectic system with an average distribution coefficient, $k_{avg.}$, considerably less than unity. Thus, the effect of P is somewhat similar to that of S. It is interesting to note there is a beneficial P-Mn interaction effect on the maximum crack length at 1% augmented strain, indicating that Mn is beneficial in minimizing the effect of P as well as that of S.

Note that there is also a detrimental S-P interaction effect. It is probable that the Ni-S-P ternary diagram, if it were available, would show even more drastic reductions in liquidus and solidus temperatures and smaller distribution coefficients than either binary system, indicating that greater degrees of segregation would occur when S and P are present together.

It is proposed, however, that S and P have an additional effect which promotes the formation of hot cracks. Figure 6 shows the etched view, utilizing Normanski phase contrast, of a crack in the specimen containing additions of S, P, and Ti. Both the location and morphology of this particular crack are unique and deserve

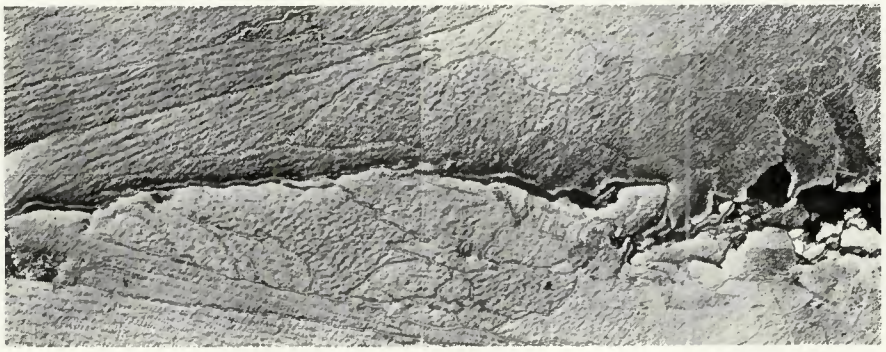

Fig. 5—Typical Hot Crack in specimen containing S (Wazau's Etch), Normarski phase contrast, ×100 (reduced 49% on reproduction)

Fig. 6—Crack at weld pad fusion line in specimen containing S, P, and Ti (Wazau's Etch), Normarski phase contrast, ×100 (reduced 50% on reproduction)

**The distribution coefficient, k, is defined as $k = C_s/C_L$, where C_s is the composition of a solid in equilibrium with a liquid of composition C_L.*

special consideration.

Note at the extreme right the fusion boundary between the weld pad and the base material. The region to the left of this line in Fig. 6 is the "pure" wrought ternary base material, while the area to the right of this line contains intentional additions of S, P, and Ti. As shown in Fig. 6, the hot crack has progressed approximately 0.085 in. (2.16 mm) (8.5 in. (216 mm) at ×100) into the pure ternary material along a network of grain boundaries. This particular treatment combination, S-P-Ti, had nearly the highest possible best value for cracking tendencies and was the only one of 64 treatment combinations which resulted in cracking in this region of the specimens during the GTA-remelting passes.

A mechanism by which such a crack could form may be summarized as follows: the progress of the GTA producing the weave bead results in highly segregated grain boundaries in the weld pad which, as shown by previous work at RPI,[7,8] must be contiguous with the boundaries in the base metal from which the growth was epitaxially nucleated. If certain energy conditions are satisfied, the segregated liquid, rich in S and P, will wet the boundaries, forming a liquid film.

The energy conditions which must be satisfied are shown in Fig 7; in order for liquid to wet the grain boundary (i.e., for $\theta = 0$), the grain-boundary energy, α_{SS}, must be greater than twice the liquid-solid interfacial energy, α_{SL}—that is, the ratio α_{SL}/α_{SS} must be less than or equal to one-half. Borland[9] suggests that low values of this ratio are extremely harmful, since nearly continuous films are formed along the boundaries. Ratios higher than 0.5 are beneficial, Borland points out, because the liquid is then restricted to grain edges and corners.

It is obvious that the ratio α_{SL}/α_{SS} must have been less than 0.5 in this case because liquid rich in S and P has penetrated along the grain boundaries in the unmelted base metal. This penetration process was undoubtedly aided by the longitudinal shrinkage stresses which would be transverse to the grain boundaries being penetrated.

With each successive pass of the arc, the situation is worsened as the one back-filled crack provides local stress relief for surrounding grain boundaries and grows progressively larger as the plate attains higher and higher temperatures. The S- and P-rich liquid thus proceeds farther each time before encountering the effective solidus isotherm.

According to this reasoning, any elements, such as P and S, which lower the surface free energy of a liquid-solid interface tend to increase the hot-cracking propensity and become the more detrimental if their distribution coefficient is small as well.

One further observation should be mentioned since it supports the proposed mechanism of formation of the crack shown in Fig. 6. It was noted during the process of Tigamajig testing, that there was a wide variation in the surface contour of the GTA spot fusion zone. In most of the specimens, the center of the top surface of the fusion zone was depressed, and the material displaced from this center region was "mounded" up around the edge of the circular GTA spot weld, as indicated in Fig. 8B.

Eight of the specimens, however, showed a relatively flat puddle surface contour, as indicated schematically in Fig. 8A. The eight specimens which showed this distinctive flat puddle surface represented the following eight treatment combinations: S, S-P, S-Al, S-Ti, S-Al-Ti, S-P-Ti, S-P-Al, and S-P-Ti-Al.

Note that this group represents all of the possible treatment combinations which contain S, and yet at the same time do not contain either Mn or Si.

One of the consequences of such a puddle contour is seen from the energy considerations shown in Fig. 8. Note that, as the puddle surface contour becomes flatter (i.e., as the angle θ approaches 0 deg, the angle α approaches 180 deg), the maximum value which the liquid-solid interfacial energy, α_{LS}, may have under equilibrium conditions must be decreased, since at equilibrium, by the law of sines:

$$\frac{\alpha_{LS}}{\sin \alpha} = \frac{\alpha_{LV}}{\sin \beta} = \frac{\alpha_{SV}}{\sin \gamma}$$

where α_{LS}, α_{LV} and α_{SV} are the surface free energies of the liquid-solid, liquid-vapor, and solid-vapor interfaces, respectively, and α, β, and γ are the angles as shown in Fig. 8.

The fact that only specimens containing S in the absence of both Mn and Si exhibited flat puddle contours provides qualitative support for the argument that S lowers the liquid-solid interfacial energy. Furthermore, on the basis of the change in surface contour in the presence of either Mn or Si, it appears highly likely that both these elements are capable of increasing the surface free energy of the solid-liquid interface, thereby minimizing boundary penetration and subsequent cracking. This argument is equally valid in explaining the effect of these elements on cracking occurring within the highly segregated structure in the remelted

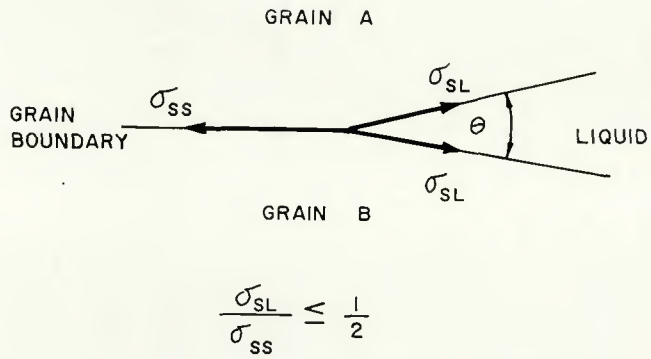

Fig. 7—Schematic representation of energy conditions required for grain-boundary wetting

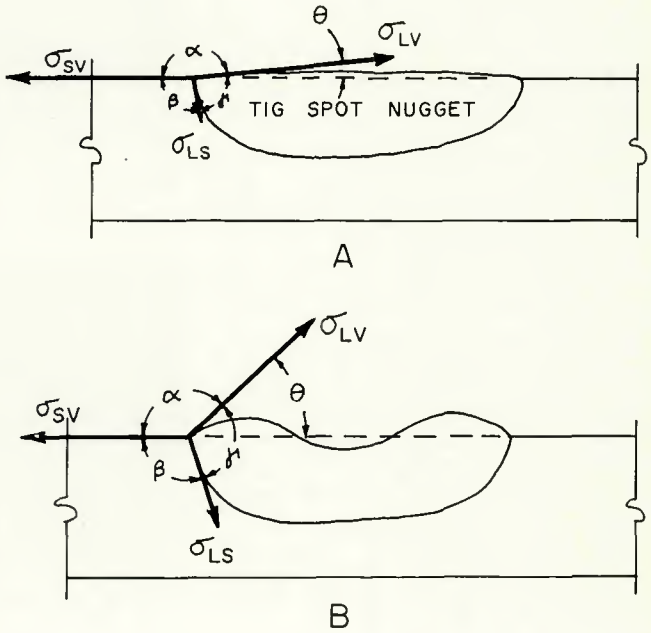

Fig. 8 (right)—Schematic view of Tigamajig fusion-zone surface contour

weld pad during Tigamajig testing—Figs. 5 and 6.

In the case of Fe-base alloys, Kiessling and Westman[10] report that the tendency for MnS to penetrate grain boundaries increases with decreasing MnS/O_2 ratio. This implies that O lowers the surface free energy of MnS, and, presumably, of S-rich liquids in general.

The oxygen content of the weld pads analyzed ranged from 0.0097 to 0.028 wt%, presumably as a consequence of the surface oxides present on the powders used in producing the air-melted base metal and those used in producing the inserts. Thus, if a similar S-O interaction occurs for Inconel, the beneficial effects of Mn, Si, Ti, and Al could also be in part a result of their strong deoxidizing capability. Unfortunately, no data are available currently on the amount of dissolved and combined O present in the weld pads, so the hypothesis cannot be verified at this time.

The Si-Mn and S-Si-Mn interactions are more difficult to explain, unless the simultaneous presence of Si and Mn results in a lower solid-liquid surface-free energy than is present with Mn alone. If the effect of a Si-Mn interaction lowering the surface free energy were to counteract part of the beneficial effects of Si on the dissolved O and of Mn when alone on the liquid-solid surface free energy, the observed effects could be rationalized.

Conclusion

The following conclusions were drawn during the evaluation of the effect of six minor alloying elements, normally present in Inconel 600, on the hot-cracking propensity of the alloy.

Method of Testing

1. The Tigamajig test was found to be a useful test for determining the susceptibility of Inconel to hot cracking, combining the virtues of the previously developed Varestraint test with a reduced specimen size and greater ease of specimen preparation.

2. It was found that the composition of Tigamajig samples could be altered and controlled within reasonable limits by the introduction of powder inserts containing the desired additions and using a series of wide-weave GTA passes to melt and mix the additions with the base metal.

3. The weave-bead technique used to incorporate the powder inserts produced a reproducible solidification substructure which was particularly sensitive to hot cracking due to the orientation of substructure boundaries with respect to the strains imposed on the Tigamajig specimen.

Choice of Cracking Parameters

1. The maximum crack length was seen to be the most sensitive indicator of cracking propensity at 1% augmented strain with the accompanying disadvantage that this parameter shows a high degree of experimental scatter. When a large number of specimens are available, the maximum crack length will reveal more significant effects, but if few samples are available, the total crack length or the average crack length will give a more reliable estimate of cracking sensitivity.

2. With regard to the strain levels, it was found that information concerning the effects on maximum crack length and average crack length is lost if testing is performed above the 1% augmented strain level, whereas increasing the augmented strain above this level produces little new information about the total crack length.

Effect of Added Elements on the Cracking Parameters for Inconel

1. S was found to have a highly detrimental effect when the avg. concentration was increased from 0.004 to 0.016 wt%. The adverse effect of S was attributed to segregation of this element and the subsequent reduction in effective solidus and liquidus, coupled with a lowering of the liquid-solid interfacial energy, causing the formation of thin films of S-rich liquid at the grain and subgrain boundaries.

2. P was found to have a detrimental effect similar to, but not as severe as, that of S when the avg. concentration of P was raised from 0.001 to 0.010%. A S-P interaction increased the detrimental effect of the two elements when both were present in combinations.

3. Mn and Si both had beneficial effects on the cracking parameters, resulting at least in part from an increase in the liquid-solid interfacial energy by the addition of these elements in the range 0.09-1.33% and 0.07–0.29%, respectively. The increase in liquid-solid interfacial energy minimizes the formation of liquid grain-boundary films, thus reducing hot-cracking propensity. Mn and Si had a detrimental interaction which limited the effectiveness of these two elements in reducing the effect of S, when both Mn and Si were present simultaneously.

4. Ti and Al also had beneficial effects on the cracking parameters investigated when Ti was increased from 0.01 to 0.32% and when Al was increased from 0.03 to 0.25%. The beneficial effect of Ti, Al, Mn, and Si was postulated to result from (in addition to the mechanism discussed above for Mn and Si) the excellent deoxidizing influence of these four elements. Since O has been observed to lower surface free energy of sulfides, it was suggested that these elements could increase the surface free energy by the reduction of dissolved O, thereby decreasing cracking tendencies.

Acknowledgment

The authors wish to acknowledge financial support provided by a NASA Traineeship during the early phase of the program.

The authors would like to acknowledge the support of the Oak Ridge National Laboratories.

References

1. Savage, W. F., and Lundin, C. D., "The Varestraint Test," *Welding Journal, 44* (10), Oct. 1965, Research Suppl., pp. 433-s to 442-s.

2. Savage, W. F., and Lundin, C. D., "Application of the Varestraint Technique to the Study of Weldability," *Welding Journal, 45* (11), Nov. 1966, Research Suppl., pp. 497-s to 503-s.

3. Davies, O. L., *The Design and Analysis of Industrial Experiments,* Hafner Publishing Company, New York, N. Y. (1960).

4. Savage, W. F., Nippes, E. F., and Goodwin, G. M., "Effect of Minor Elements on Fusion-Zone Dimensions of Inconel 600," *Welding Journal,* to be published.

5. Cochran, W. G., and Cox, G. M., *Experimental Designs,* John Wiley & Sons, Inc., New York, N. Y. (1957).

6. Bowker, A. H., and Lieberman, G. J., *Engineering Statistics,* Prentice-Hall, Inc., Englewood Cliffs, N. J. (1959).

7. Savage, W. F., and Aronson, A. H., "Preferred Orientation in the Weld Fusion Zone," *Welding Journal, 45* (2), Feb. 1966, Research Suppl., pp. 85-s to 89-s.

8. Savage, W. F., Lundin, C. D., and Chase, T. F., "Solidification Mechanics of Fusion Welds in Face-Centered Cubic Metals," *Welding Journal, 47* (11), Nov. 1968, Research Suppl., pp. 522-s to 526-s.

9. Borland, J. C., "Suggested Explanation of Hot Cracking in Mild and Low Alloy Steel Welds," B.W.R.A. Report, *Welding Research Abroad,* VIII, 2, Feb. 1962.

10. Kiessling, R., and Westman, C., "Sulfide Inclusions and Synthetic Sulfides of the (Mn, Mo)S-Type," *Journal of the Iron and Steel Institute, 204* (4), 377-379, 1966.